Nanotechnology for Environmental Engineering (2022) 7:57–66
https://doi.org/10.1007/s41204-021-00186-1

ORIGINAL PAPER

Adsorption and photocatalytic performance of ZnAl layered double hydroxide nanoparticles in removal of methyl orange dye

Vijayalaxmi D. Thite[1] · **Sushama M. Giripunje**[1]

Received: 28 July 2021 / Accepted: 7 November 2021 / Published online: 1 February 2022

Abstract
The textile industries generate huge amounts of highly toxic color wastewater. A potential solution to this global environmental pollution demands the appropriate design and synthesis of artificial photocatalysts with high activities. The presence of methyl orange (MO) dye causes distinct acute impact on health therefore the removal of this dye from aqueous solution is highly desirable. The aim of this study was to assess the efficiency of photo-degradation of methyl orange dye with application of ZnAl layered double hydroxides (LDHs) as a photocatalyst. For this purpose, ZnAl LDHs were synthesized by simple and cost-effective coprecipitation method with varying Zn/Al molar ratios 2:1, 3:1 and 4:1. Samples were characterized by XRD, TG–DTA and UV–visible techniques to achieve information in aspects of phase transformation, thermal stability and their dye absorption capacity. Crystallinity and bandgap of catalyst play an important role in dye degradation mechanism & it is observed that the crystallinity of LDHs increases on calcination (at 600°C) and Zn/Al molar ratio. The investigation also reveals that an increase in Zn/Al molar ratio and calcination influences the dye degradation capacity of catalyst. It was found that the photocatalytic activity of calcined ZnAl LDHs depends on its intermediate products ZnO and $ZnAl_2O_4$ composites which can be regulated by changing Zn/Al molar ratio and heat treatment. The highest degradation of MO dye was found to be 95.21% within a time period of 1 h. Also, the reusability and stability of ZnAl photocatalyst were found to be steady up to 5 successive cycles.

Keywords Methyl orange (MO) dye · ZnAl layered double hydroxide (LDH) · Dye degradation · Photocatalyst · Calcination

Introduction

A rapidly growing population followed by development of modern industry paved the way for environmental pollution through hazardous wastes leading to global health and environmental risk. The organic pollutants, dyes and pigments in water even at very low concentrations are highly toxic and they can produce some potential carcinogens, which will be harmful to humans and animals as well as the whole ecosystem. There is emerging public concern over the contamination of wastewater by dyes. Nowadays, there are more than 10,000 types of commercially used dyes. More seriously, about 1–20% of these dyes are lost during the dyeing process and they are released as textile effluents. Facing the ever-growing demand for eco-friendly wastewater management without affecting urbanization, research is recently devoted to the search of natural dyes from plants, animals and minerals which can be renewable having less impact on environmental resources [1]. Biological method alone cannot effectively degrade dyes from wastewater hence use of chemicals become essential. The methods used for dye removal are adsorption, encapsulation, degradation, etc. [2–4]. Among these potential solutions, photocatalysis has emerged as a fascinating technique because it is economic, non-toxic, safe and renewable. In the photocatalytic process, sunlight illumination can be utilized as an energy source. Selection of photocatalyst depends on the nature of dye and quantity of contamination. Synthetic textile dyes have complex aromatic molecular structures that make them difficult to biodegrade when discharged in the ecosystem. Owing to this, the design and synthesis of artificial photocatalysts with high activities have attracted great scientific interest worldwide.

✉ Sushama M. Giripunje
sushama_3sep@yahoo.co.in

[1] Department of Physics, Visvesvaraya National Institute of Technology, Nagpur 440010, India

Layered double hydroxide (LDH) is a widely used multifunctional material due to its physical & chemical properties, excellent stability as well as its non-toxicity, great accessibility and moderate cost. LDHs have been used as catalysts specially adsorbents in case of many aquatic pollutants as they are excellent ion exchangers. LDH fits in class of doped semiconductors and because of its interchangeable laminate elements, the semiconductor properties can be tailored by varying laminate cations and interlaminar anions [5]. Because of high anion retention capacity and simple thermal regeneration procedure LDHs materials are used as photocatalysts [6–8]. Electron–hole pairs are generated through the irradiation of light on catalyst surface which undergo oxidation or reduction of the pollutants in the solution [9]. $[MII_{1-x}MIII_x(OH)_2]_x^+[A^{n-}_{x/n} \cdot y.H_2O]_x^-$ where M(II) and M(III) are divalent and trivalent metal cations, respectively, and A^{n-} is an n-valent anion. Substitution of M^{2+} by M^{3+} leaves the positive charge which is then neutralized by intercalating anion and held by hydrogen bonding[10]. ZnAl-LDHs have been proved to have good capacity for wastewater treatment due to the outstanding synergism of adsorption and photocatalysis [11–13].

ZnO is one of the widely used photocatalysts for environmental pollution problems due to its high photosensitivity, non-toxic nature, low cost and chemical stability [14], some studies show higher activity of ZnO than TiO_2 [15–18]. However, the principal limitation of using ZnO is a quick recombination of the photogenerated (e − /h +) pairs. Few researchers had tried to rectify this limitation by modifying the structure or doping of ZnO [19, 20]. Moreover, in few reports, it is found that the use of ZnO for the production of H_2 is possible, but the results are not are very favorable due to the low yield of H_2 [21–25]. On the other hand, the oxides obtained from the calcined LDH materials at different temperatures are highly active in the photodegradation of organic pollutants [6, 13, 16, 25]. In case of ZnAl LDH containing Zn as one of the metal cations, it is possible to obtain composite materials based on ZnO and ZnAl mixed oxides by only calcination. It is a cheap and simple alternative to the other routes such as ceramic, wet chemical synthesis or doping of ZnO with Al by magnetron sputtering, pulsed laser deposition (PLD), chemical vapor deposition (CVD), chemical bath deposition (CBD) and spray pyrolysis (SP) [7, 19, 22].

The photocatalytic degradation efficiency of organic dyes depends on the phase structure of catalyst which in turn depends on the calcination temperature. Many studies found that the calcination of LDH material influences their photocatalytic activity due to the formation of mixed metal oxide and their composites [8–10, 26–32]. ZnAl LDH structures intercalated with carbonate ions and modified with Sn^{4+} cations have been studied for the photocatalytic degradation of organic compounds by Mendoza-Damián, G. et al.[33]. Also, the influence of different interlayer anions on the electron structure and surface chemical state of ZnAl–LDH structure through the experimental verification was investigated by Huo, Wangchen et al.[34].

Experimental

Materials

Zinc chloride ($ZnCl_2$), aluminum chloride hexahydrate ($AlCl_3.6H_2O$), sodium carbonate (Na_2CO_3) and sodium hydroxide (NaOH) have been purchased from Merck-Germany & Sigma-Aldrich-USA. All the used chemicals were of analytical grade and were used without further purification.

Synthesis of ZnAl LDH nanoparticles

ZnAl LDHs nanoparticles were synthesized by a versatile and cost-effective co-precipitation method in which supersaturation of cation and anion leads to homogeneous nucleation followed by seed-assisted growth of nucleus. Three 60 ml solutions of $ZnCl_2$ and $AlCl_3.6H_2O$ at specific molar ratios 2:1(pH 3), 3:1(pH 2) and 4:1(pH 1) were prepared and basic solution NaOH containing Na_2CO_3 was added to it until the pH of solution become 5. During this process, the solution was continuously stirred at 1300 rpm for homogeneous mixing. The solution was transferred to Teflon lined stainless steel autoclave for heat treatment at 70 °C for 7 h. Resulting suspension was centrifuged and then dried at room temperature (≈27 °C), thus ZnAl LDH powder samples were obtained and were labeled as Z2A, Z3A and Z4A for Zn:Al ratio as 2:1(pH 3), 3:1(pH 2) and 4:1(pH 1), respectively. To avoid contamination of the sample due to formation of CO_3^{-2} all reagents were stored in N2 filled glove box and the synthesis was also carried out in the same glove box. Samples were calcinated at optimized temperature 600 °C. These calcinated samples were labeled as Z2AC, Z3AC and Z4AC for 2:1, 3:1 and 4:1 Zn:Al ratio, respectively.

Photocatalytic activity evaluation

The degradation of methyl orange (MO) dye using ZnAl LDH catalyst was investigated by monitoring degradation efficiency for fixed time intervals. A handmade photo reactor containing a single incandescent lamp (40 W/230 V Philips Intensity approx. 24,000 lx) was used as the simulated sunlight source which was kept at 12 cm from the base of the round bottom flask containing mixture of dye and catalyst with continuous stirring on a magnetic stirrer. To maintain constant temperature (28 °C) of the reaction system running water was circulated through the jacket. For photocatalytic

degradation 0.03 gm of synthesized ZnAl LDH catalyst was added to 100 ml aqueous solution of MO dye with 10 ppm concentration. This mixture was stirred continuously for 1 h in dark to achieve its adsorption–desorption equilibrium. Then 5 ml of aliquot was collected and centrifuged to separate catalyst particles and the supernatant solution was used for UV analysis. In the next step, 5 ml aliquot was collected after each 15 min of irradiation and used for UV analysis. The percentage degradation efficiency (DE %) was calculated using Eq. (1).

$$\mathrm{DE}\% = \frac{C_0 - C_t}{C_0} \times 100 \quad (1)$$

where C_0 is the initial concentration of dye solution and Ct is the dye concentration at reaction time t.

Optimization of catalyst concentration for dye degradation

From the obtained results, it was found that the degradation of MO dye increased with the increase in the concentration of catalyst. This could be due to the generation of hydroxyl radicals. The generation of hydroxyl radicals increases with an increase in catalyst dosage. About 95.21% of MO dye was decolorized with the loading of 0.3 $g\,L^{-1}$ of catalyst over 60 min irradiation. On increasing the catalyst dosage, the total active surface area escalates, that eventually tends to availability of additional active sites. The other reason could be, on increasing the catalyst dosage, the collision frequency between the catalyst and dye increases. Concurrently the increase in catalyst dosage may lead to an increase in turbidity. At higher turbidity, the passage of UV light into the solution diminishes and ultimately decreases the photoactivity.

Characterizations

The crystalline structure of ZnAl LDH was recorded by X-Ray diffractometer with CuKα radiation ($k = 0.154059$ nm) at a scan rate of 2°/min to determine the crystallite size. The diffraction pattern was recorded with a step size of 0.03. The effect of calcination on the percent weight loss was analyzed using thermogravimetric analysis (TG–DTA-7200 Hitachi). Particle size determination and lattice fringe observation were performed using high-resolution transmission electron microscope (HR-TEM,300 kV). A double beam UV–Vis–NIR spectrophotometer (JASCO V-670) was used to study the absorption spectra of the samples.

Results and discussion

X-ray diffraction (XRD) study

Figure 1a & b illustrate the XRD pattern of ZnAl LDHs with different Zn/Al cationic ratio and their calcined products, respectively. Characteristic reflections have been observed corresponding to (003), (006), (012), (015), (018) diffraction planes. The sharpness and symmetry of these reflections indicate a high crystalline LDH phase. Considering the hexagonal

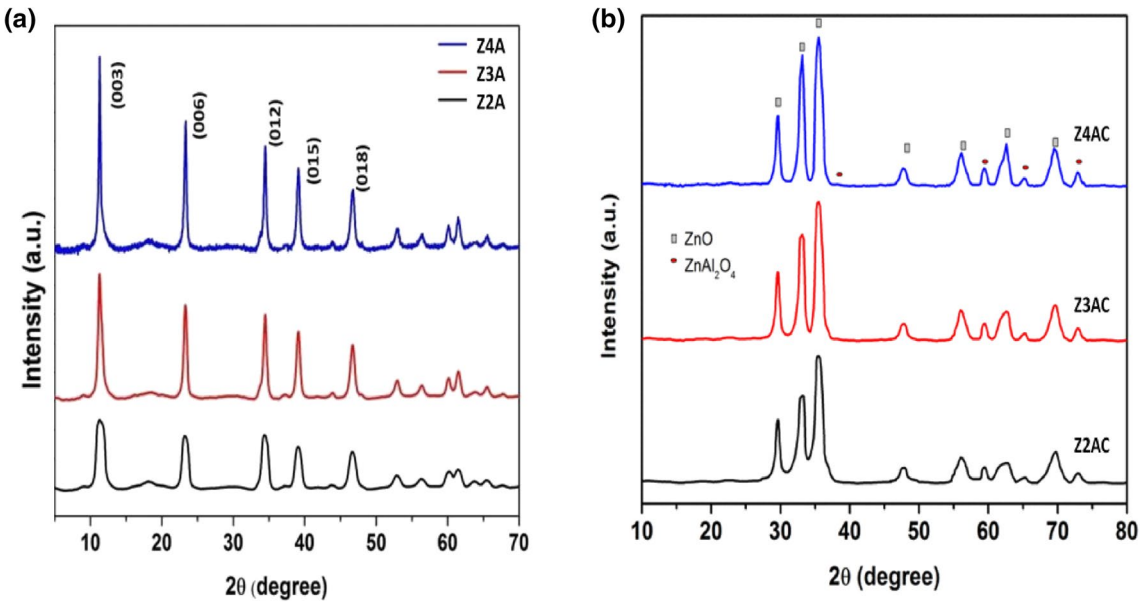

Fig. 1 X-ray diffractograms of **a** ZnAL LDHs and **b** calcined ZnAl LDH

packing, the lattice parameters a and c were calculated using (003) and (110) reflecting planes. Parameter **a** represents the average metal–metal distance in the interlayer structure which was calculated from the position of (110) plane. Parameter **c** corresponds to three times the interlayer distance which was determined from the position of (003) reflection. These lattice parameters were found to be $a=b=0.37$ nm & $c=2.46$ nm. After calcination, the lamellar structure collapse and the new peaks corresponding to ZnO oxide and $ZnAl_2O_4$ spinel phases were observed as shown in Fig. 1b [42]. Characteristic reflections of the composite ZnO/ $ZnAl_2O_4$ appear at 600 °C. By increasing Zn/Al molar ratio amount of ZnO/ $ZnAl_2O_4$ composite also increases. Scherrer's formula [Eq. (2)] was used to calculate the crystallite size and it was found to be 27.2 nm for Z4AC, 24.6 nm for Z3AC and for Z2AC it reduces to 19 nm. Scherrer's formula is expressed as.

$$D = \frac{k\lambda}{\beta \cos\theta} \tag{2}$$

where k is shape factor (0.9), λ is the X-ray wavelength (Cu/ Kα = 0.154 nm), β is the full width at half-maximum of the diffraction peak and θ is the angle of diffraction. From Fig. 1b the diffraction peaks at 31.59°, 34.18°, 36.12°, 47.44°, 56.50°, 62.65° and 68.07° reflect the structure of ZnO and the diffraction peaks at higher 2° values 44.69°, 59.09°, 65.07° and 77.04° corresponds to $ZnAl_2O_4$. The presence of zinc aluminate diffraction peaks and the slightly shifted peaks of ZnO represent the incorporation of zinc aluminate into ZnO resulting in the formation of $ZnAl_2O_4$/ ZnO nanocomposite due to calcination of ZnAl LDH.

TEM analysis

To investigate the morphology and particle size distribution of prepared sample, TEM analysis was performed. TEM image Fig. 2a demonstrates that the particles are spherical with agglomeration. From the particle size distribution graph shown in Fig. 2b, the average particle size of Z4AC was found to be 44.28 nm. From the inset of Fig. 2c, SAED (Selected area electron diffraction) pattern of Z4AC exhibits three uniform rings with bright spots which reveal nanocrystalline nature of Z4AC. The diffraction rings of the sample are indexed to (400) and (101) planes corresponding to $ZnAl_2O_4$ and ZnO, respectively, which confirms the formation of $ZnAl_2O_4$/ZnO nanocomposite. Figure 2d shows the lattice fringe spacing of 0.25 nm corresponding to (110) plane of the ZnO crystallites.

TGA-DTA analysis

Figure 3 shows the TG–DTA curve of ZnAl LDH nanoparticles. The mass loss in temperature range 40–180 °C is attributed to water loss from inter- and intra-gallery of LDH structure and also from some externally absorbed water. Decomposition and elimination of organic moiety and removal of OH from hydroxide layer also cause mass loss. Second stage of mass loss at higher temperatures between 200 °C and 500 °C is due to the dehydroxylation of the brucite-like sheets as well as the decomposition of the carbonate anions. The mass loss above 500 °C corresponds to dehydration and dehydroxylation of AlOOH. [41]. At 600 °C and above the weight loss was not so significant and the formation of spinel phase initiates.

UV–Visible spectroscopy

Generation and migration of photoexcited electron–hole pairs tailor the probability of their presence at reaction sites on the photocatalyst surface. Hence the optical absorption is the key factor in the regulation of photocatalytic reaction mechanism. The optical energy bandgap was calculated by using standard Eq. (3).

$$\alpha h\nu = (h\nu - Eg)/2 \tag{3}$$

where α, ν, k and Eg are the absorption coefficient, light frequency, the proportionality constant and the bandgap, respectively. Characteristic transition represented by 'n' is 1or 3 for direct transition and 4 or 6 for an indirect transition.

The effect of phase transformations after calcination of ZnAl LDHs on their capability to absorb visible light was examined. As shown in Fig 4a & b calcined Z4AC catalyst shows absorption in visible region and uncalcined Z4A catalyst shows absorption at the edge of visible region, indicating that the bandgap of catalyst decreases after calcination. Thus the calcined catalyst showed significant absorption in visible region and decreased bandgap value due to formation of ZnO/ $ZnAl_2O_4$ nanocomposite during calcination. A possible mechanism for the degradation of methyl orange is supposed that $ZnAl_2O_4$ and ZnO in ZnO/ $ZnAl_2O_4$ catalyst are coupled together and their conduction band (CB) and valence band (VB) levels are showing a good match. The energy gap between corresponding band levels drives the e^- and h^+ pairs from one particle to its neighbors to form a spatial separation. Such process is energetically favorable for photogenerated e − and h + pairs. The resulting O2 − and OH − ions get oxidized by photogenerated holes (h +) to generate the free radicals ·O2 − and OH· which are responsible for the degradation of methyl orange. This can be visualized with Fig. 5.

Photocatalytic study

The performance of calcined and uncalcined ZnAl LDHs as photocatalyst can be evaluated from the degradation of MO dye under visible light irradiation. For experiment,

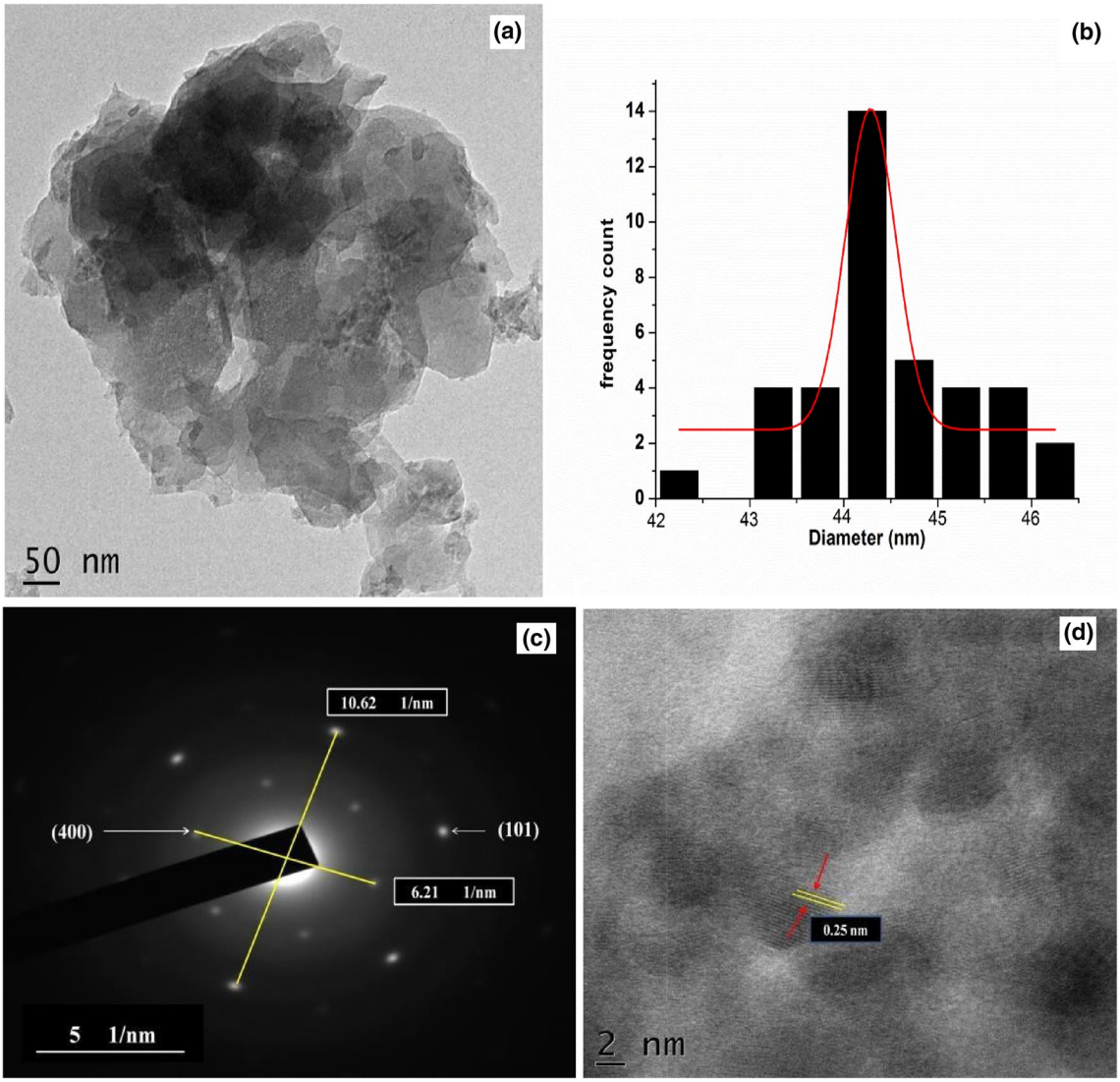

Fig. 2 **a** HR-TEM images **b** average particle size distribution **c** SAED pattern **d** lattice fringe spacing of Z4AC

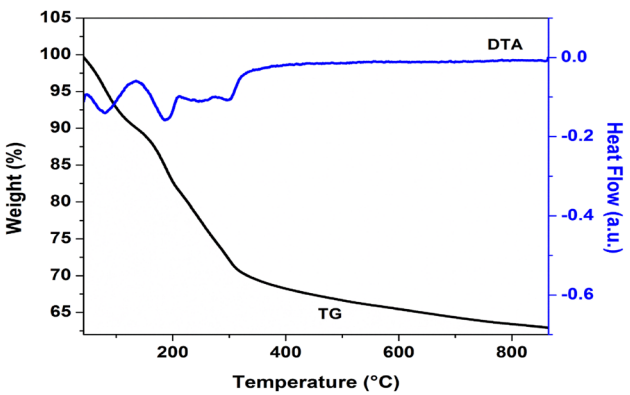

Fig. 3 TG–DTA curves of Z4AC

10 ppm aqueous solution of MO dye was prepared in 100 ml double distilled water. This solution was stirred in dark for an hour to reach its adsorption–desorption equilibrium and then irradiated with visible light for 15 min. 5 ml of resultant solution was pipette out and centrifuged to study its optical absorption after every 15 min interval. The change in MO dye adsorption was monitored with the help of UV–Vis spectra. It was observed that adsorption increases with the increase in Zn/Al molar ratio. This may be due to the increased crystallinity of ZnO phase with an increased Zn/Al molar ratio. Also, in case of Z4A sample, there was the formation of ZnO phase due to increase in Zn content. Also, the effect of calcined catalyst on degradation shows desired results. Figure 6a & b show the change in degradation efficiency of MO dye with duration of irradiation from which it is clear that all the calcined catalysts

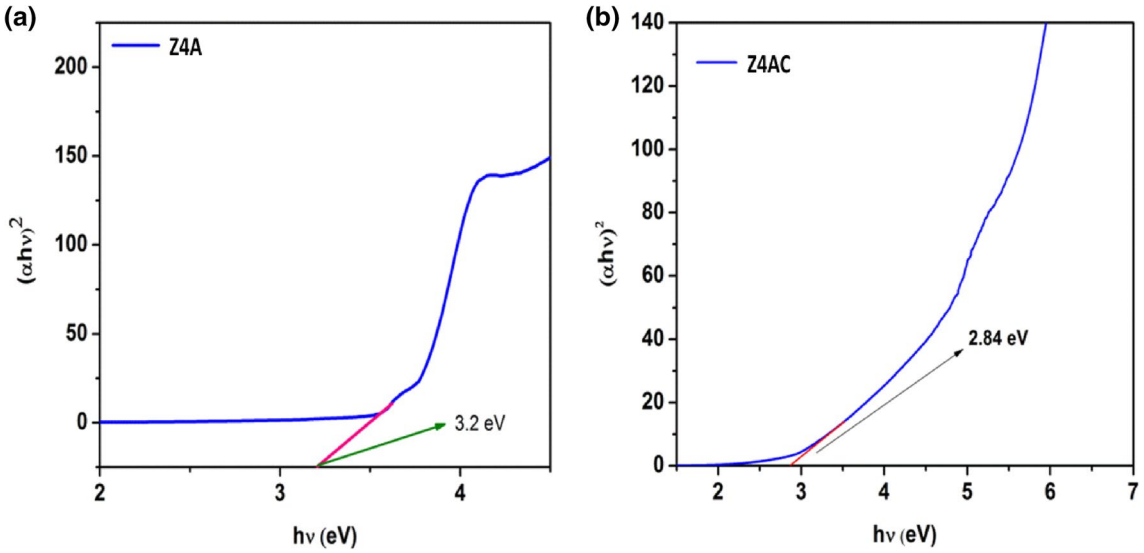

Fig. 4 **a** UV–Vis spectra of Z4A LDH sample **b** UV–Vis spectra of calcined Z4AC LDH sample

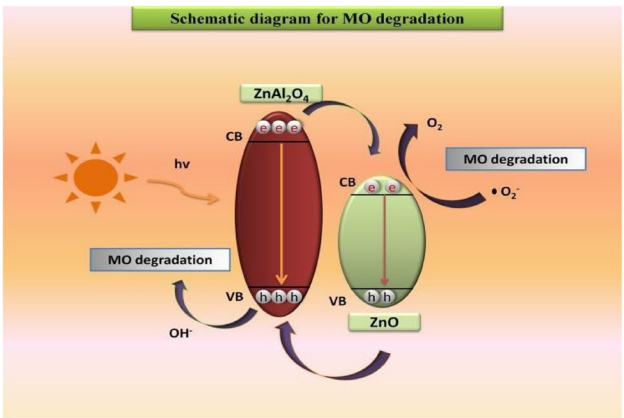

Fig. 5 Schematics of different energy levels coupling action in ZnO and $ZnAl_2$

samples achieved higher degradation rate than uncalcined catalysts. Calcination process caused the coupling of ZnO and $ZnAl_2O_4$ nanocomposites which ensures the effective separation of photogenerated electron–hole pairs, which is an important factor to enhance photocatalytic performance of a single-phase material. Reaction conditions as shown in Fig. 6c demonstrate the kinetics of MO dye degradation. It evaluates the photocatalytic degradation of dyes as a function of irradiation time. LDHs role in dye degradation can be explained on the basis of Langmuir–Hinshelwood Model [42–44] which is expressed by Eq. (4).

$$r = -\frac{dC}{dt} = \mathrm{KKrC} = \mathrm{KappC} \tag{4}$$

where r is dye degradation rate, K refers to the adsorption equilibrium constant, Kr is the reaction rate constant, Kaap is the apparent rate constant and C is dye concentration in solution. At initial condition of photocatalytic degradation ($t=0$, $C=C_o$) this equation becomes first-order kinetic equation when C is very less, then Eq. (4) becomes

$$\ln\frac{C_0}{C} = \mathrm{Kappt} \tag{5}$$

where C_0 initial dye concentration, C is dye concentration at time t and Kaap is the apparent rate constant, respectively. The rate constant Kaap = 5 E^{-2} min^{-1} calculated by using Eq. (5) is the gradient of graph ln (C/Co) versus irradiation time as shown in Fig. 6c. From the investigation and results shown in Fig. 6a & b, sample Z4A shows maximum adsorption–desorption equilibrium in 60 min with 89.74% dye degradation, where Z4AC degrades 95.21% dye in 60 min. Thus we can conclude that calcined LDHs have higher degradation efficiency than uncalcined LDHs. The absorption spectra of MO dye solution in presence of Z4AC catalyst are shown in Fig. 6d. On the other hand, a comparative study of the effect of changing molar ratio of Zn/Al in LDH on its photocatalytic performance leads to the conclusion that the increasing Zn/Al molar ratio in LDH also increases its photocatalytic performance. This is due to increased crystallinity and increasedZnO/ $ZnAl_2O_4$ nanocomposites.

$$\mathrm{ZnO} - \mathrm{ZnAl_2O_4} + h\nu \rightarrow \mathrm{ZnO}\left(e^- + h^+\right) + \mathrm{ZnAl_2O_4}\left(e^- + h^+\right) \tag{6}$$

$$\mathrm{ZnO}\left(e^- + h^+\right) + \mathrm{ZnAl_2O_4}\left(e^- + h^+\right) \rightarrow e^-(\mathrm{ZnO}) + h^+\left(\mathrm{ZnAl_2O_4}\right) \tag{7}$$

$$e^- + O_2 \rightarrow O_2^{-\cdot} \tag{8}$$

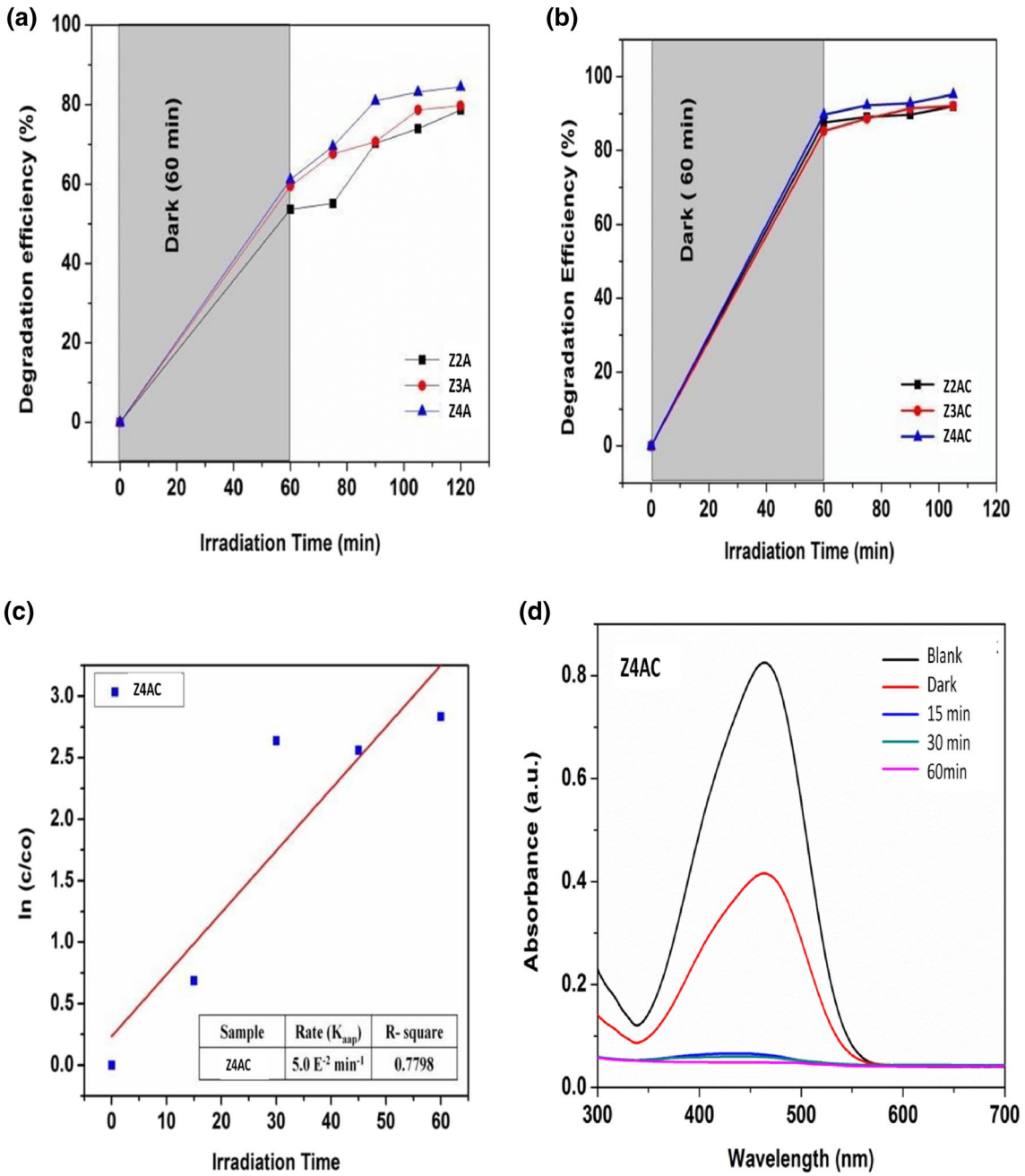

Fig. 6 **a** Kinetic study of MO dye degradation for sample Z4AC. **b** Degradation efficiencies of Z2A, Z3A, Z4A samples for MO dye. **c** Degradation efficiencies of Z2AC, Z3AC, Z4AC samples for MO dye. **d** Change in the absorption of 10 ppm MO dye solution in Z4AC under irradiation. The tentative mechanism of MO dye degradation can be explained as follows

$$2\,e^- + O_2 + 2H^+ \rightarrow H_2O_2 \quad (9)$$

$$e^- + H_2O_2 \rightarrow OH^\bullet + OH^- \quad (10)$$

$$h^+ + OH^- \rightarrow OH^\bullet \quad (11)$$

$$MO(dye) + OH^\bullet \rightarrow \text{Dye product} \quad (12)$$

$$O_2^{-\cdot} + \text{Mo (dye)} \rightarrow \text{Dye product} \quad (13)$$

When ZnAl LDH/MO aqueous solution irradiates with photon energy greater than the bandgap of ZnAl LDHs

nanoparticles, it produces electron–hole pair in LDH as expressed in Eqs. (6 & 7). Superoxide O2-· anion radicals are generated by the combination of an electron from the conduction band with dissolved oxygen from environment (Eq. (8)). These superoxides further react with dye to produce dye products (Eq. (13)). Electron further reacts with dissolved oxygen and proton to form hydrogen peroxide (H2O2) which reacts with photoelectron (Eq. (9)) leading to the generation of hydroxyl radicals (OH·) Eq. (10)). Similarly, holes from the VB oxidize the H2O molecule to hydroxyl radicals (OH·) as given in Eq. (11). These OH· radicals are strongly oxidizing which degrade the MO dye (Eq. (12)).

To understand the dye degradation mechanism and radicals involved, trapping experiment was carried out by using scavengers like benzoquinone(BQ) for $O_2^{-}\cdot$, isopropanol(IPA) for $OH^{\bullet}$ and sodium oxalate for h^{+}. As perceived in Fig. 7a, photodegradation of IC dye was considerably suppressed by using BQ in which degradation efficiency decreased from 95.21% to 28.49%, and by addition of IPA, it reduced to 63.15%. While the addition of sodium oxalate slightly promotes(95.53%) the degradation efficiency as it acts as electron donor that reacts with holes at catalyst surface, which in turn inhibits the recombination rate of photogenerated electron–hole pairs. From the overall trapping experiment, it was clear that $O_2^{-}\cdot$ and $OH^{\cdot}$ radicals are responsible for MO dye degradation.

The reusability of Z4AC LDH catalyst was investigated by using same experimental conditions for repeated cycles. The catalyst was separated after each cycle and washed several times with distilled water and dried at 60° overnight to reuse for photocatalytic degradation of MO dye. Figure 7b reveals that Z4AC is a recyclable and highly stable catalyst for MO dye degradation upto five successive cycles. After 16 cycles catalyst totally lost its degradation efficiency (Table 1).

Conclusion

ZnAl LDHs with several Zn/Al molar ratios 2:1, 3:1 and 4:1, as photocatalyst were synthesized by co-precipitation method. We investigated the LDHs phases based on zinc and aluminum metals and interspersed by carbonate ions represented as Zn-Al-CO3. The effect of calcination of LDHs on degradation efficiency for MO dye has been investigated. While experimentation we optimized the calcination temperature to 600 °C and observed that during the calcination, the material transform into mixed metal oxides (ZnO-$ZnAl_2O_4$). ZnAl LDHs calcined at 600 °C and for Zn/Al molar ratio 4:1(Z4AC) showed the best removal rate of MO dye about 95.21% within a time period of 1 h. All LDHs samples before and after calcination were characterized by several physicochemical techniques such as XRD, TEM, UV–Vis, PL, etc. The study revealed that crystallinity and bandgap play an important role in dye degradation capacity of catalyst. Also the reusability and stability of Z4AC photocatalyst were found to be steady up to 5 successive cycles. Thus this synthetic anionic clay in the form of photocatalyst presents a remarkable performance to be used as an efficient adsorbent for the removal of hazardous MO dye from an aqueous solution/wastewater.

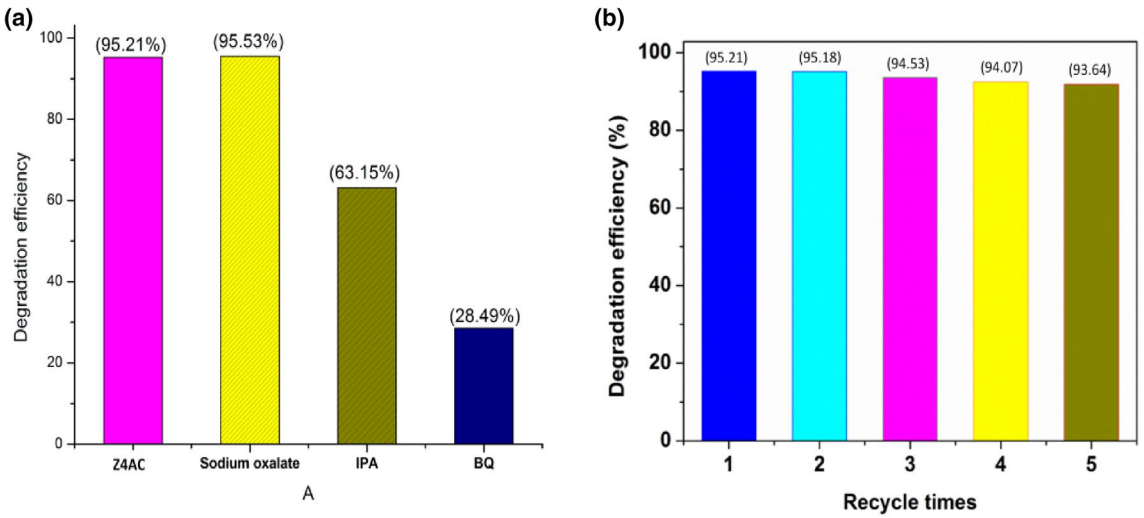

Fig. 7 **a** Trapping experiment analysis **b** Reusability of catalyst Z4AC

Table 1 List of Publications relevant to LDHs photocatalyst

Author	Year	Findings	Source	Reference no
Hongo, Teruhisa, Takeshi Iemura and Atsushi Yamazaki	2008	Adsorption ability for several harmful anions and thermal behavior of Zn-Fe layered double hydroxide	*Journal of the Ceramic Society of Japan*	*46*
Marangoni, Rafael, et al	2009	Zn2Al layered double hydroxides intercalated and adsorbed with anionic blue dyes: A physico-chemical characterization."	*Journal of colloid and interface science*	*41*
Dvininov, E., et al. "	2010	New SnO2/MgAl-layered double hydroxide composites as photocatalysts for cationic dyes bleaching."	*Journal of Hazardous Materials*	*32*
Shao, Mingfei, et al	2011	The synthesis of hierarchical Zn–Ti layered double hydroxide for efficient visible-light photocatalysis	*Chemical Engineering Journal*	*33*
Xia, Sheng-Jie, et al	2013	"Layered double hydroxides as efficient photocatalysts for visible-light degradation of Rhodamine B."	*Journal of colloid and interface science*	*47*
Seftel, E. M., et al. "	2015	Photocatalytic removal of phenol and methylene-blue in aqueous media using TiO2@ LDH clay nanocomposites."	*Catalysis Today*	*56*
Zhang, Yan, Shuai Jing and Hongyuan Liu	2015	Reactivity and mechanism of bromate reduction from aqueous solution using Zn–Fe (II)–Al layered double hydroxides."	*Chemical Engineering Journal*	*35*
Fei, Weihua, et al	2019	"Fabrication of visible-light-active ZnO/ZnFe-LDH heterojunction on Ni foam for pollutants removal with enhanced photoelectrocatalytic performance."	*Solar Energy*	*45*

References

1. Sponza DT, Işık M (2004) Decolorization and inhibition kinetic of Direct Black 38 azo dye with granulated anaerobic sludge. Enzyme Microb Technol 34(2):147–158
2. Kassem AA et al (2020) Hydrogenation reduction of dyes using metal-organic framework-derived CuO@C. Microporous Mesoporous Mater 305:110340
3. Abdelhamid HN (2020) Dye encapsulated hierarchical porous zeolitic imidazolate frameworks for carbon dioxide adsorption. J Environ Chem Eng 84:104008
4. Georgouvelas D et al (2021) All-cellulose functional membranes for water treatment: Adsorption of metal ions and catalytic decolorization of dyes. Carbohyd Polym 264:118044
5. Wang Y et al (2018) Cobalt-doped Ni–Mn layered double hydroxide nanoplates as high-performance electrocatalyst for oxygen evolution reaction. Appl Clay Sci 165:277–283
6. Xue Y et al (2018) Relationship of cellulose and lignin contents in biomass to the structure and RB-19 adsorption behavior of activated carbon. New J Chem 42(20):16493–16502
7. Figueiredo JL et al (2011) Adsorption of dyes on carbon xerogels and templated carbons: influence of surfacechemistry. Adsorption 17(3):431–441
8. Se EM (2015) el, M. Niarchos, C. Mitropoulos, M. Mertens, EF Vansant and P. Cool. Catal Today 252:120–127
9. Selcuk H (2005) Decolorization and detoxification of textile wastewater by ozonation and coagulation processes. Dyes Pigm 64(3):217–222
10. De Gisi S et al (2016) Characteristics and adsorption capacities of low-cost sorbents for wastewater treatment: a review. Sustain Materi Technol 9:10–40
11. Starukh G (2017) Photocatalytically enhanced cationic dye removal with Zn-Al layered double hydroxides. Nanoscale Res Lett 12(1):391
12. Abderrazek K, Najoua FS, Srasra E (2016) Synthesis and characterization of [Zn-Al] LDH: study of the effect of calcination on the photocatalytic activity. Appl Clay Sci 119:229–235
13. Seftel EM, Popovici E, Mertens M, Witte KD, Tendeloo GV, Cool P, Vansant EF (2008) Zn-Al layered double hydroxides: synthesis, characterization and photocatalytic application. Microporous Mesoporous Mater 113(1–3):296–304
14. Hernández-Alonso MD et al (2009) Development of alternative photocatalysts to TiO 2: challenges and opportunities. Energy Environ Sci 212:1231–1257
15. Tzompantzi F et al (2011) Improved photocatalytic degradation of phenolic compounds with ZnAl mixed oxides obtained from LDH materials. Top Catal 54(1–4):257–263
16. Tzompantzi F et al (2014) Enhanced photoactivity for the phenol mineralization on ZnAlLa mixed oxides prepared from calcined LDHs. Catal Today 220:56–60
17. Zhang Li et al (2013) Fabrication and photocatalytic properties of spheres-in-spheres ZnO/ $ZnAl_2O_4$ composite hollow microspheres. Appl Surface Sci 268:237–245
18. Yuan X et al (2017) Photocatalytic Cr (VI) reduction by mixed metal oxide derived from ZnAl layered double hydroxide. Appl Clay Sci 143:168–174

19. Lee KM et al (2016) Recent developments of zinc oxide based photocatalyst in water treatment technology: a review. WaterRes 88:428–448
20. Edalati K et al (2016) Low-temperature hydrothermal synthesis of ZnO nanorods: effects of zinc salt concentration, various solvents and alkaline mineralizers. Mater Res Bull 74:374–379
21. Zhang Li et al (2014) Photocatalytic degradation and inactivation of Escherichia coli by ZnO/ZnAl2O4 with heteronanostructures. Transs Nonferrous Metals Soc China 243:743–749
22. Reli M et al (2015) Photocatalytic H2 generation from aqueous ammonia solution using ZnO photocatalysts prepared by different methods. Int J Hydrogen Energy 40.27:8530–8538
23. Luévano-Hipólito E, Torres-Martínez LM (2017) Sonochemical synthesis of ZnO nanoparticles and its use as photocatalyst in H2 generation. Mater Sci Eng B 226:223–233
24. Vickers NJ (2017) Animal communication: when i'm calling you, will you answer too? Curr Biol 27(14):R713–R715
25. Guan MY et al (2013) ZnO/ $ZnAl_2O_4$ prepared by calcination of ZnAl layered double hydroxides for ethanol sensing. Sensors Actuators B Chem 188:1148–1154
26. Armijo F et al (2007) Electrocatalytic oxidation of nitrite to nitrate mediated by Fe (III) poly-3- aminophenyl porphyrin grown on five different electrode surfaces. J Molecular Catal A Chem 26812:148–154
27. Dvininov E et al (2010) New SnO2/MgAl-layered double hydroxide composites as photocatalysts for cationic dyes bleaching. J Hazard Mater 177(1–3):150–158
28. Shao M et al (2011) The synthesis of hierarchical Zn–Ti layered double hydroxide for efficient visible-light photocatalysis. Chem Eng J 168(2):519–524
29. Smith JT et al (2004) Measurement of cell migration on surface-bound fibronectin gradients. Langmuir 20(19):8279–8286
30. Zhang Y, Jing S, Liu H (2015) Reactivity and mechanism of bromate reduction from aqueous solution using Zn–Fe (II)–Al layered double hydroxides. Chem Eng J 266:21–27
31. Mendoza-Damián G et al (2016) Improved photocatalytic activity of SnO2–ZnAl LDH prepared by one step Sn4+ incorporation. Appl Clay Sci 121:127–136
32. Huo W et al (2019) Anion intercalated layered-double-hydroxide structure for efficient photocatalytic NO remove. Green Energy Environ 4(3):270–277
33. Chuang YH et al (2008) Removal of 2-chlorophenol from aqueous solution by Mg/Al layered double hydroxide (LDH) and modified LDH. Ind Eng Chem Res 47.(11):3813–3819
34. Kameda T et al (2009) Preparation of Mg–Al layered double hydroxides intercalated with alkyl sulfates and investigation of their capacity to take up N, N-dimethylaniline from aqueous solutions. Solid State Sci 11(12):2060–2064
35. Marangoni R et al (2009) Zn2Al layered double hydroxides intercalated and adsorbed with anionic blue dyes: a physico-chemical characterization. J Colloid Interface Sci 333(1):120–127
36. Liu S et al (2014) Active oxygen-assisted NO-NO2 recycling and decomposition of surface oxygenated species on diesel soot with Pt/Ce0.6Zr0.4O2 catalyst. Chinese J Catal 35(3):407–415
37. Nejati K et al (2018) Zn–Fe-layered double hydroxide intercalated with vanadate and molybdate anions for electrocatalytic water oxidation. New J Chem 42(4):2889–2895
38. Rahmanian O, Amini S, Dinari M (2018) Preparation of zinc/iron layered double hydroxide intercalated by citrate anion for capturing Lead (II) from aqueous solution. J Mol Liq 256:9–15
39. Hongo T, Iemura T, Yamazaki A (2008) Adsorption ability for several harmful anions and thermal behavior of Zn-Al layered double hydroxide. J Ceram Soc Jpn 116(1350):192–197
40. Pavia DL, Lampman GM, Kriz GS (1976) Introduction to organic laboratory techniques. A contemporary approach, Saunders Golden Sanburst Series, pp 599–614
41. Koyani RD et al (2013) Contribution of lignin degrading enzymes in decolourisation and degradation of reactive textile dyes. Int Biodeteriorat Biodegradat 77:1–9
42. Husain Q (2010) Peroxidase mediated decolorization and remediation of wastewater containing industrial dyes: a review. Rev Environ Sci Bio/Technol 9(2):117–140
43. Crini G (2006) Non-conventional low-cost adsorbents for dye removal: a review. Biores Technol 97(9):1061–1085
44. Alvim RS et al (2014) Theoretical chemistry at the service of the chemical defense: Degradation of nerve agents in magnesium oxide and hydroxide surface. Rev Virtual Quim 20(19):687–723
45. Smith JT et al (2004) Measurement of cell migration on surface-bound fibronectin gradients. Langmuir 20(19):8279–8286